An Early Investigation of Ytterbium Nanocolloids for Selective and Quantitative "Multicolor" Spectral CT Imaging

Dipanjan Pan,[†,*] Carsten O. Schirra,[‡] Angana Senpan,[†] Anne H. Schmieder,[†] Allen J. Stacy,[†] Ewald Roessl,[§] Axel Thran,[§] Samuel A. Wickline,[†] Roland Proska,[§] and Gregory M. Lanza[†]

[†]C-TRAIN and Division of Cardiology, Washington University School of Medicine, 4320 Forest Park Avenue, St. Louis, Missouri 63108, United States, [‡]Philips Research North America, 345 Scarborough Road, Briarcliff Manor, New York 10510, United States, and [§]Philips Research Europe—Hamburg, Röntgenstrasse, D-22335 Hamburg, Germany

ABSTRACT

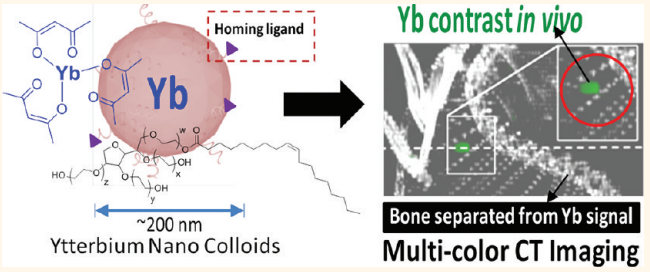

We report a novel molecular imaging agent based on ytterbium designed for use with spectral "multicolor" computed tomography (CT). Spectral CT or multicolored CT provides all of the benefits of traditional CT, such as rapid tomographic X-ray imaging, but in addition, it simultaneously discriminates metal-rich contrast agents based on the element's unique X-ray K-edge energy signature. Our synthetic approach involved the use of organically soluble Yb(III) complex to produce nanocolloids of Yb of noncrystalline nature incorporating a high density of Yb (>500K/nanoparticle) into a stable metal particle. The resultant particles are constrained to vasculature (~200 nm) and are highly selective for binding fibrin in the ruptured atherosclerotic plaque. Nanoparticles exhibited excellent signal sensitivity, and the spectral CT technique uniquely discriminates the K-edge signal (60 keV) of Yb from calcium (bones). Bioelimination and preliminary biodistribution reflected the overall safety and defined clearance of these particles in a rodent model.

KEYWORDS: ytterbium · nanoparticle · spectral CT imaging · contrast agent · multicolor imaging · thrombus

Atherosclerosis is the single largest "clinically silent" killer of men and women in the United States and considered as the primary basis of coronary artery disease (CAD). CAD is a progressive disease process that generally begins in early days and manifests clinically in adulthood, expressing atherosclerotic changes within the walls of the coronary arteries. It is now well-established that the acute formation of thrombus following atherosclerotic plaque rupture is the origin of myocardial infarction.[1,2] Although a myriad of medical advances in coronary imaging have since emerged, particularly computed tomography coronary angiography, the ability to diagnose ruptured plaque in vessels with only 50−60% residual stenosis continues to be challenging.[3−8] The emergence of "multicolor" energy-resolved computed tomography (CT), also referred to as spectral CT, in combination with K-edge metal contrast agents is poised to provide unequivocal advantages for rapid diagnosis and quantification of intracoronary thrombus associated with ruptured plaque in the ED.[3−8]

Spectral CT is the newest in a series of CT imaging advances, including multidetector CT (MDCT) and dual-energy CT. Unlike integrating detectors for traditional and dual-energy CT, spectral CT commonly employs dedicated detectors capable of counting single X-ray photons and discriminating their energy into three or more energy windows (bins). With the obtained plurarity of energy-selective measurements, certain metals can be exclusively and quantitatively imaged without background signal by uniquely recognizing their K-edge discontinuity in the attenuation cross section. Hitherto, a number of heavy metals for K-edge imaging have been investigated, such as gold[9] and bismuth.[10] In a phantom study, the potential use of iodine and gadolinium for simultaneous imaging of two metals was demonstrated.[11]

A unique challenge in the design and synthesis of targeted spectral CT agents, as opposed to blood pool contrast agents, is

* Address correspondence to dipanjan@wustl.edu.

Received for review January 26, 2012 and accepted March 4, 2012.

Published online March 04, 2012
10.1021/nn300392x

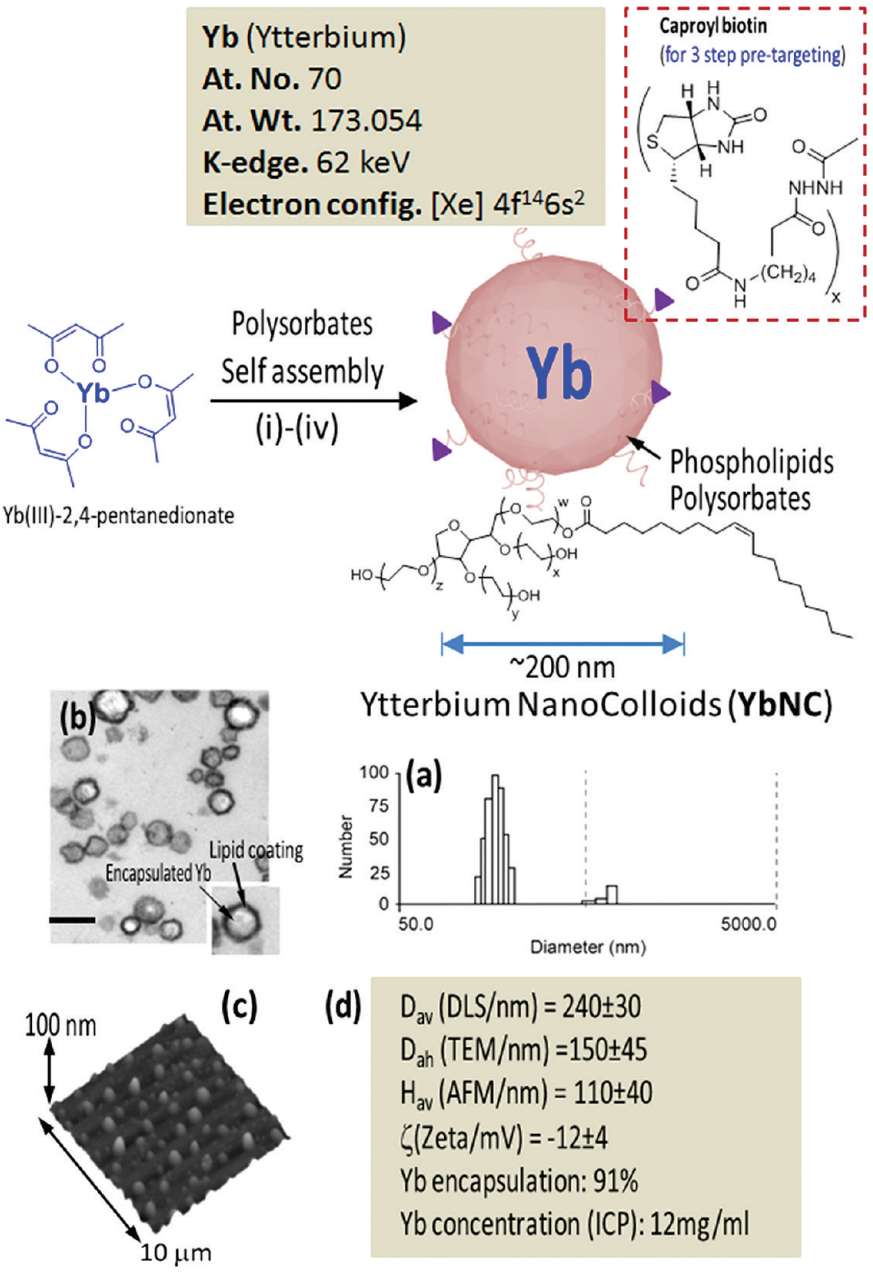

Figure 1. Synthesis and physicochemical characterization of self-assembled ytterbium nanocolloids (YbNC). Schematic describing the preparation of Yb-enriched YbNC: (i) suspension of Yb(III) 2,4-pentanedionate in polyoxyethylene (20) sorbitan monooleate, vigorously vortexed and mixed, filtered using cotton bed, vortexex; (ii) preparation of phospholipid thin films composed of egg lecithin PC; (iii) resuspension of the thin film in water (0.2 μM); (iv) microfluidization at 4 °C, 20 000 psi (141 MPa), 4 min, dialysis (cellulosic membrane, MWCO 20K); characterization table for a representative preparation of YbNC. (a) Number-averaged hydrodynamic diameter distribution of YbNC. (b) TEM images of the lipid-encapsulated nanocolloids. (c) AFM image of YbNC drop deposited over glass grid. (d) Physicochemical characterization chart.

the requirement of enormously high metal content (*ca.* 500 000 metal atoms/nanoparticle) to achieve measurable concentrations with the given density of binding sites.[10] Although iodine is the cornerstone of conventional blood pool CT contrast agents, for spectral CT applications in humans, the low K-edge of iodine (Z = 53, K = 33.2 keV) is predicted through modeling to suffer from photon starvation and consequently yield poor noise properties in the K-edge image.[12] Although gold (Z = 79, K = 80.7 keV) is attractive for its high atomic number and K-edge energy, the cost of this precious metal required for human diagnostic studies will essentially preclude its commercial translation to the clinic. We have shown that vascular-constrained nanoparticles (160 nm) incorporating a bismuth organometallic core (Z = 83, K = 89.5 keV) offer an attractive metal with high atomic number. Fibrin-targeted organobismuth nanoagents have been demonstrated to be effective for imaging clot phantoms *in vitro* and intraarterial thrombus in the rabbit iliac artery *in vivo*.[10]

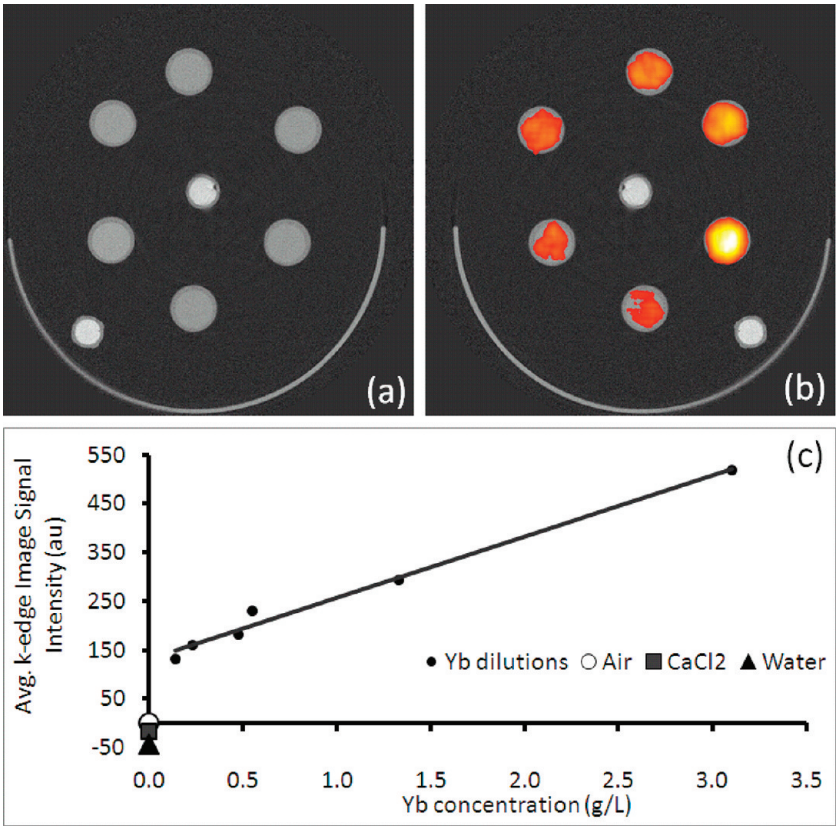

Figure 2. While conventional CT renders an image providing information about the overall attenuation, commonly represented in Hounsfield units (a), spectral CT is capable of separating the K-edge information and selectively imaging ytterbium (b). The Yb K-edge signals (red-yellow) were overlaid on the traditional CT image of YbNC dilutions, a water and $CaCl_2$ sample (gray). The signal intensity from serial dilutions of YbNC shows a linear correlation to Yb concentrations obtained by ICP-OES (c), which makes spectral CT a quantitative imaging technique.

However, while these preliminary results are promising, the absorption profile of bismuth is not optimal for K-edge imaging.[12]

Simulations, considering a spectral CT system as realized in the prototype spectral CT system utilized in the experiments, indicate that heavy metals with atomic numbers between approximately 60 and 65 yield optimal noise performance.[12] Gadolinium ($Z = 64$, $K = 50.2$ keV) shows significantly higher X-ray contrast enhancement (43.1 HU/mg Gd/mL at 120 keV) than iodine (32.1 HU/mg I/mL at 120 keV). However, the association of this metal with nephrogenic systemic fibrosis, combined with unsuccessful attempts to formulate self-assembled Gd nanocolloids from Gd-2,4-pentanedionate, advises the use of other metals for K-edge imaging. Depending on the range of incident X-ray spectrum, which is typically in the range of 60−130 kV, and the composition and diameter of the scanned object, the signal-to-noise ratio (SNR) in the K-edge channel depends strongly on the metal. For a clinical setup, metals with atomic numbers around 70 are ideal. Ytterbium is ($Z = 70$, $K = 61.3$ keV) perfectly positioned to yield high SNR. In its chelated form, Yb was once considered as a CT blood pool contrast agent and was found to have a favorable safety profile with a high LD_{50} in rodents.[13−15] In the present research, we hypothesize that high payloads of the Yb in the form of hydrophobic small molecule metal complexes could be designed and stably concentrated into lipid-encapsulated nanocolloids.

RESULTS AND DISCUSSION

Metal clusters (*e.g.*, fcc structure) of Yb were synthesized previously by the bioreduction method to generate high metal content, particularly as blood pool agents.[16] However, their large size (*i.e.*, >6 nm), the renal clearance threshold, and resultant poor biological elimination pose potential issues regarding long-term safety, similar to the barriers facing quantum dots or carbon nanotubes (SWNT). Very recently, Lu *et al.* reported an Yb-based nanoparticle stabilized with oleic acid and modified with the biocompatible polymer DSPE-PEG 2000 for conventional CT imaging.[17] However, to the best of our knowledge, the use of ytterbium as a nanoparticulate spectral "multicolor" CT contrast agent has not been previously reported. The design of these particles involved concentrating a hydrophobic Yb complex (ytterbium(III) 2,4-pentanedionate) within a phospholipid-entrapped intravascular colloidal nanoparticle (>150 nm).

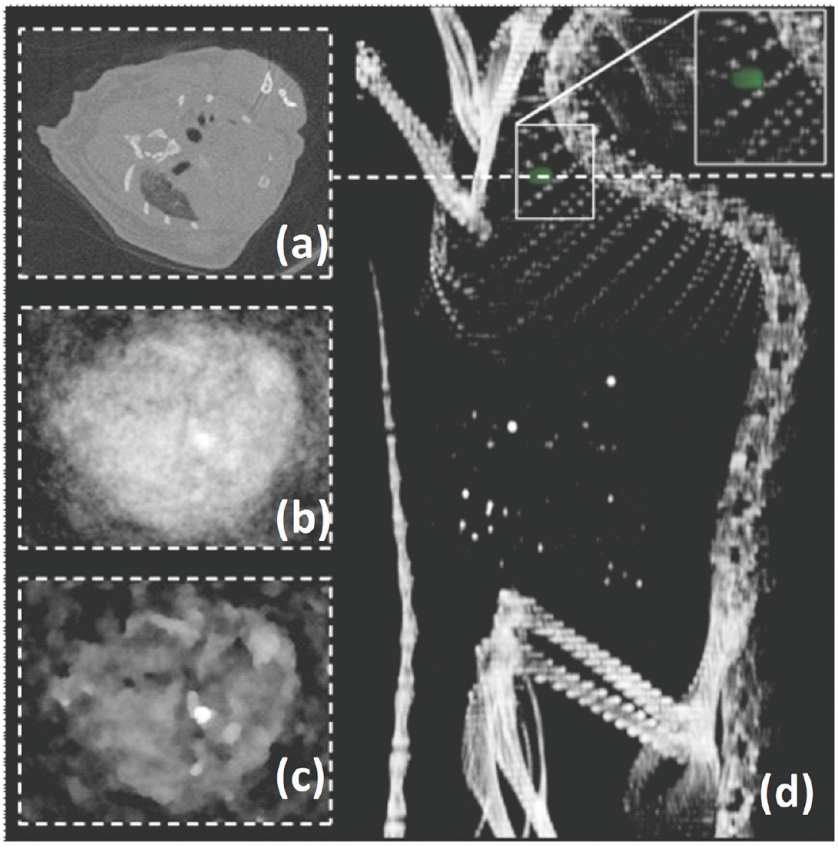

Figure 3. Blood pool imaging in mouse after bolus application of nontargeted Yb nanocolloids (6 mL/kg). (a) Pseudoconventional CT image composed from spectral measurements, slice through heart (dashed line). Statistical image reconstruction of Yb signal after 1 (b) and 20 iterations. (c) Volume rendered conventional CT image with super-positioned Yb signal (green) shows accumulation of Yb in the heart and the clear separation from bone (d).

Self-assembled Yb nanocolloids were prepared from organically soluble trivalent ytterbium complex suspended in polysorbate. The core was encapsulated in a phospholipid monolayer through high-pressure homogenization. Briefly, the synthesis process involved suspending commercially available ytterbium(III) 2,4-pentanedionate in polyoxyethylene (80) sorbitan monooleate followed by microfluidization as a 20% (v/v) colloidal suspension with a 2% (v/v) phospholipids surfactant in nanopure water (Figure 1).

The surfactant mixture comprised phosphatidylcholine (lecithin-egg PC, 99 mol %) and dipalmitoyl phosphatidylethanolamine caproyl biotin (1 mol % w/v, PE-biotin) for *in vitro* avidin−biotin coupling of homing ligands. YbNC was purified by exhaustive dialysis through 10 kDa MWCO membrane against nanopure water (0.2 μM) (Figure 1). Multiple syntheses resulted in colloidal nanoparticles with a mean particle size of 240 $\pm$ 30 nm using dynamic light scattering with zeta-potentials in the range of −12 to −18 mV and low polydispersity (<0.2). In a typical preparation, ytterbium content was determined by ICP-OES, as 0.41 mg/mL of the 20% colloidal suspension, which corresponded to approximately 1200K Yb atoms/nanoparticle with 1.1 $\times$ 10^{12} particles/mL. The Yb nanoparticles vialed and sealed under argon have exhibited significant shelf-life stability with <7% change in hydrodynamic diameter and polydispersities over 2 months at 4 °C.

The nanoparticles were further characterized in the anhydrous state by transmission electron microscopy (TEM) and atomic force microscopy (AFM). For TEM, Yb nanoparticles were fixed with 2.5% glutaraldehyde and sequentially stained with osmium tetroxide and tannic acid before embedding in Polybed812. Poststained in uranyl acetate and lead citrate, these particles were imaged on an electron microscope (JEOL 100CX) and observed to be spherical with a distinct dark lipid periphery (Figure 1b). AFM particle height was 110 $\pm$ 40 nm, reflective of their compressible nature.

A prototype spectral CT system (Philips Research, Hamburg, Germany) utilizing a single-slice, photon-counting detector featuring six energy bins (Gamma Medica Inc., Northridge, California, USA) was used to evaluate the Yb nanocolloids. In an initial experiment, YbNC in aqueous suspension was imaged. Figure 2a shows a representative cross section of the experimental setup rendered as a conventional CT image. It shows a pattern of X-ray lucent tubes filled with serially diluted YbNC suspension (YbNC:H_2O, 1:2, 1:4, 1:8, 1:16, 1:32, 1:64) and two additional reference tubes filled with agarose and calcium chloride, respectively. Using spectral CT

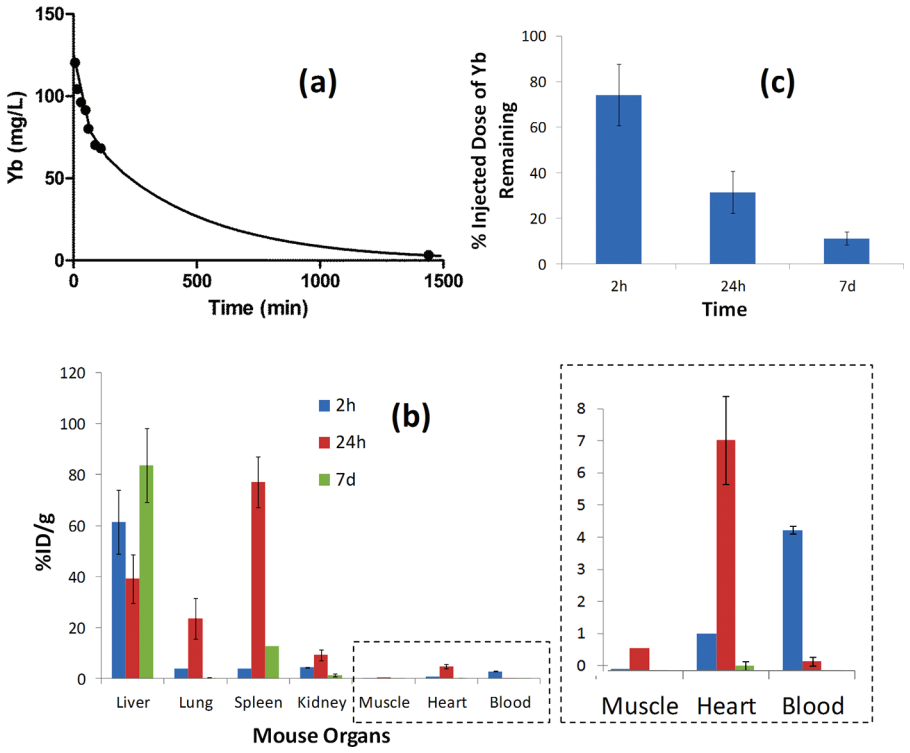

Figure 4. ***In vivo*** **pharmacokinetics, biodistribution, and clearance of YbNC in mouse. (a) Pharmacokinetic profile of nontargeted YbNC with a biexponential fit [$y = 0.0456 \times \exp(-0.0391x) + 0.1022 \times \exp(-0.0018x)$]. (b) Organ distribution of YbNC based on ytterbium estimation of major organs by ICP-OES at 2 h, 24 h, and 7 days following intravenous injection of YbNC (1 mg/mL). (c) Whole body clearance of YbNC showing only** ***ca.*** **11% remaining after 7 days post-YbNC administration.**

processing tools, the acquired data was decomposed individually into its photoelectric absorption, Compton effect, and K-edge components. The obtained ytterbium-selective image was then superimposed using color-coding (yellow, high concentration; red, low concentration) on the conventional CT image (Figure 2b). Absolute Yb concentrations derived from the K-edge image were compared with the concentrations obtained by inductively coupled plasma optical emission spectrometry (ICP-OES), revealing a good linear correlation between both results (Figure 2c; $R^2 = 0.987$). This allows linear mapping of concentrations to the ytterbium image, which makes spectral CT a quantitative imaging technique.

The detection sensitivity of the prototype spectral CT scanner has been significantly improved through recent developments in the image reconstruction technique from the usual algorithms of filtered back projection to statistical image reconstruction techniques.[18] The applicability of this technique for Yb imaging was conceptually tested using a mouse blood pool study. In this preliminary study, the animal was briefly anesthetized with isoflurane to effect and injected with YbNC (150 μL) into the tail vein. Two minutes later, the animal was euthanized and the blood pool was imaged for the metal with spectral CT. The scan parameters were as follows: tube voltage 130 kV, tube current 50 μA, threshold energies 25−46−61−64−76−91 keV, views per turn 900, rotation time 72 s, slice increment 0.5 mm, reconstructed FOV 60 × 60 mm^2, pixel size 0.1 × 0.1 mm^2.

Figure 3a shows a representative cross section through the heart. While a change in contrast due to Yb is barely visible in the conventional CT image (Figure 3a), the K-edge image using spectral CT and iterative reconstruction presents the YbNC with a high signal-to-noise ratio (Figure 3b,c). To the best of our knowledge, this represents the first spectral CT imaging with Yb nanoparticles. Owing to the sensitivity limitations of the spectral CT system, only high concentrations in the heart were successfully separated from background noise. With ongoing improvements of the spectral CT prototype, low concentrations as envisioned in the vascular system are expected to become visible in the future. The lack of spectral CT signal from other major organs can be explained due to the relatively short circulation time (2 min after intravenous administration) of the YbNC. Although more in-depth *in vivo* experiment is warranted in the future, this preliminary experiment demonstrates that YbNC can be successfully imaged with spectral CT at a concentration when the contrast was barely visible with conventional CT.

The pharmacokinetics and biodistribution of these particles were studied in a mouse model. Following intravenous injection (25 μL), the concentration of ytterbium in serial blood samples as a function of time was

determined by ICP-OES (Figure 4a). Pharmacokinetic profiles of YbNC followed a two-compartment biexponential model ($y = 40.9 \times e^{(-0.028x)} + 84.1 \times e^{(-0.002x)}$). The half-lives were 25.2 and 303 min for the distribution and clearance phases, respectively. Biodistribution of YbNC was determined by analyzing the major organs following intravenous administration of YbNC (25 μL) in mice at 2 h, 24 h, and 7 days (n = 3/time point) using ICP-OES. These results were consistent with the expected clearance of the particle through the reticuloendothelial system (RES) as evident by the high organ uptake in liver, spleen, and kidney. Interestingly, the relatively high accumulation of YbNC in liver has been noticed, which is not typically observed in this type of colloidal nanoparticles. Further detailed investigation is warranted to study the *in vivo* biodistributive properties of these particles. Finally, the whole body bioelimination of the YbNC (25 μL i.v.) was tested in mice at 2 h, 24 h, and 7days (n = 3/time point). These data showed approximately 90% elimination of the metal over the 7 day study, with 11 $\pm$ 3% remaining at that time.

Spectral CT holds great potential for a broad range of clinical applications, such as breast cancer screening and kidney stone characterization, but we anticipate that the initial major impact of the technology will be for molecular imaging beginning with the urgent diagnosis of acute coronary syndrome in EDs.

CONCLUSIONS

Overall, these data conceptually demonstrate the potential use of YbNC as targeted spectral CT contrast agents. YbNC were produced by facile synthesis of small organo-metallic molecules that were predominately bioeliminated within a week of intravenous injection. Yb, by virtue of its high atomic number and a well-positioned K-edge, provides excellent spectral CT contrast *in vitro* and *in vivo*. The potential of these particles to be homed to biological targets, particularly fibrin deposits, supports further development of these particles for intracoronary detection of non-occlusive microthrombus associated unstable ruptured plaque in patients presenting with chest pain of potential cardiac etiology. A preliminary biodistribution and clearance study shows that intravenously delivered nanoparticles are presumably taking a RES route for clearance from the body, which can be predicted for similar particles.

METHODS

Unless otherwise listed, all solvents and reagents were purchased from Aldrich Chemical Co. (St. Louis, MO) and used as received. Anhydrous chloroform was purchased from Aldrich Chemical Co. and distilled over calcium hydride prior to use. Biotinylated dipalmitoyl phosphatidylethanolamine and high purity egg yolk phosphatidylcholine were purchased from Avanti Polar Lipids, Inc. Cholesterol and sorbitan sesquioleate were purchased and used as received from Aldrich Chemical Co. (St. Louis, MO). Ytterbium(III) 2,4-pentanedioante was purchased from Spectrum Chemicals, Inc. and used as received. Argon and nitrogen (UHP, 99.99%) were used for storage of materials. The Spectra/Por membrane (cellulose MWCO = 10 000 Da) used for dialysis was obtained from Spectrum Medical Industries, Inc. (Laguna Hills, CA).

Preparation of Ytterbium Nanocolloids. YbNCs were prepared by suspending a solution of ytterbium(III) 2,4-pentanedionate (Aldrich Chemicals, Inc., 0.3 g in chloroform) in sorbitan mono-9-octadecenoate poly(oxy-1,2-ethanediyl (5 mL, Aldrich Chemicals, Inc.), and the mixture was vortexed vigorously to homogeneity. The chloroform was evaporated away under reduced pressure at 80 °C. The surfactant comixture included high-purity egg phosphatidylcholine (lecithin-egg PC, 99 mol %, 398 mg) and dipalmitoyl phosphatidylethanolamine caproyl biotin (1 mol % w/v, PE-biotin, ~2 mg). The surfactant comixture was dissolved in chloroform, evaporated under reduced pressure, dried in a 50 °C vacuum oven overnight, and dispersed into water by probe sonication. This suspension was combined with the ytterbium polysorbate mixture (20% v/v) and distilled with deionized water (77.3% w/v) and glycerin (1.7%, w/v). The mixture is continuously processed thereafter at 20 000 psi for 4 min with an S110 Microfluidics emulsifier. The nanoparticles were dialyzed against water using a 10 000 Da MWCO cellulose membrane for prolonged period of time and then passed through a 0.45 μm Acrodisc syringe filter. The nanocolloids were stored under argon atmosphere at 4 °C.

Dynamic Light Scattering Measurements. Hydrodynamic diameter distribution and distribution averages for the biotinylated YbNC and controls in aqueous solutions were determined by dynamic light scattering. Hydrodynamic diameters were determined using a Brookhaven Instrument Co. (Holtsville, NY) Model Zeta Plus particle size analyzer. Measurements were made following dialysis (MWCO 10 kDa dialysis tubing, Spectrum Laboratories, Rancho Dominguez, CA) of YbNC suspensions into deionized water (0.2 mM). Nanoparticles were dialyzed into water prior to analysis. Scattered light was collected at a fixed angle of 90°. A photomultiplier aperture of 400 mm was used, and the incident laser power was adjusted to obtain a photon counting rate between 200 and 300 kcps. Only measurements for which the measured and calculated baselines of the intensity autocorrelation function agreed to within +0.1% were used to calculate nanoparticle hydrodynamic diameter values. All determinations were made in multiples of five consecutive measurements.

Electrophoretic Potential Measurements. Zeta-potential (z) values for the YbNCs were determined with a Brookhaven Instrument Co. (Holtsville, NY) model Zeta Plus zeta-potential analyzer. Measurements were made following dialysis (MWCO 10 kDa dialysis tubing, Spectrum Laboratories, Rancho Dominguez, CA) of YbNC suspensions into water. Data were acquired in the phase analysis light scattering (PALS) mode following solution equilibration at 25 °C. Calculation of z from the measured nanoparticle electrophoretic mobility (ζ) employed the Smoluchowski equation $\mu = \varepsilon\zeta/\eta$, where ε and η are the dielectric constant and the absolute viscosity of the medium, respectively. Measurements of ζ were reproducible to within $\pm$4 mV of the mean value given by 16 determinations of 10 data accumulations.

Stability of the Nanocolloids. Preliminary long-term storage stability of the nanocolloids was assessed by measuring hydrodynamic diameter distributions over a period of >60 days from the time of synthesis for different replicates of YbNC formulations preserved under inert atmosphere (*i.e.*, argon) at 4 °C. Changes in particle size and polydispersity indexes due to Ostwald ripening were minimal (<7%) over the observation period.

Inductively Coupled Plasma Optical Emission Spectroscopy. The ytterbium (Yb) content of YbNC was analyzed by inductively

coupled plasma optical emission spectroscopy (ICP-OES, Perkin-Elmer Optima 7000). The samples were treated with a mixture of concentrated nitric acid, concentrated hydrochloric acid, and hydrogen peroxide followed by digestion using Multiwave 3000 (Anton Paar, USA).

Spectral CT Imaging. The spectral CT prototype scanner and data processing method employed in our studies has been previously reported[5,6] for imaging phantoms. The attenuation was decomposed into photoeffect, Compton effect, and ytterbium. The scan parameters were set as follows: tube voltage 130 kV, tube current 50 μA, threshold energies 25−46−61−64−76−91 keV, views per turn 900, rotation time 72 s, slice increment 0.5 mm, reconstructed FOV 60 × 60 mm^2, pixel size 0.1 × 0.1 mm^2.

***In Vivo* Imaging and Biodistribution.** Guidelines on the care and the use of laboratory animals at Washington University in St. Louis were followed for all animal experiments. Initial anesthetization of mouse was done using a mixture of ketamine (85 mg/kg) and xylazine (15 mg/kg) and maintained on 0.75−1.0% isoflurane delivered through a calibrated vaporizer. YbNC was administered intravenously through tail vein catheter. In this preliminary study, the animal was briefly anesthetized with isoflurane to effect and injected with YbNC (150 μL) into the tail vein. Two minutes later, the animal was euthanized and the blood pool was imaged for the metal with spectral CT. For *in vivo* pharmacokinetics and biodistribution of YbNC in mouse, YbNC was administered (1 mL/kg; total volume) intravenously through a tail vein catheter in mice (n = 3 each time point). After 2 h, 24 h, and 7 days post-YbNC administration, the major organs were independently frozen, ground to tissue homogeneity, weighed, and the entire specimen was analyzed for Yb content using ICP-OES. Pharmacokinetic profile of nontargeted YbNC followed a biexponential curve fit.

Bioelimination Study. Six mice were devided in three groups and received YbNC (1 mL/kg) *via* intravenous catheter. Of the six treated mice, two mice were sacrificed 2 min after intravenus injection to establish the maximum whole body concentration of Yb. Subsequently, four mice were sacrificed from the remaining four animals on days 7 and 14 postinjection. Carcasses of all animals were independently frozen, ground to tissue homogeneity, weighed, and the entire specimen was submitted for Yb content analysis using ICP-OES. No adverse effects were observed in these animals during the in-life phase of the study, which indicated the lack of free Yb bioavailability from the metal complex.

Conflict of Interest: The authors declare no competing financial interest.

Acknowledgment. This research was supported by grants from the AHA (0835426N and 11IRG5690011), NIH (R01CA154737, R01HL094470, R01NS059302, UO1NS073457), and NCI (U54CA119342). We also thank M. Levy (Cell Biology) for helping us with TEM experiments.

REFERENCES AND NOTES

1. Benson, R. The Present Status of Coronary Arterial Disease. *Arch. Pathol. Lab. Med.* **1926**, *2*, 876–916.
2. Constantinides, P. Plaque Fissures in Human Coronary Thrombosis. *J. Atheroscler. Res.* **1966**, *6*, 1–17.
3. Kelly, J. L.; Thickman, D.; Abramson, S. D.; Chen, P. R.; Smazal, S. F.; Fleishman, M. J.; Lingam, S. C. Coronary CT Angiography Findings in Patients without Coronary Calcification. *AJR Am. J. Roentgenol.* **2008**, *191*, 50–55.
4. Tong, L. L. Poor Correlation between Coronary Artery Calcification and Obstructive Coronary Artery Disease in an End-Stage Renal Disease Patient. *Hemodial. Int.* **2008**, *12*, 16–22.
5. Taylor, A. J. A Comparison of the Framingham Risk Index, Coronary Artery Calcification, and Culprit Plaque Morphology in Sudden Cardiac Death. *Circulation* **2000**, *101*, 1243–1248.
6. Pham, P. H. Computed Tomography Calcium Quantification as a Measure of Atherosclerotic Plaque Morphology and Stability. *Invest. Radiol.* **2006**, *41*, 674–680.
7. Barreto, M. Potential of Dual-Energy Computed Tomography To Characterize Atherosclerotic Plaque: *Ex Vivo* Assessment of Human Coronary Arteries in Comparison to Histology. *J. Cardiovasc. Comput. Tomogr.* **2008**, *2*, 234–242.
8. Horiguchi, J.; Fujioka, C.; Kiguchi, M.; Shen, Y.; Althoff, C. E.; Yamamoto, H.; Ito, K. J. Soft and Intermediate Plaques in Coronary Arteries: How Accurately Can We Measure CT Attenuation Using 64-MDCT? *Am. Roentgenol.* **2007**, *189*, 981–988.
9. Cormode, D.; Roessl, E.; Thran, A.; Skajaa, T.; Gordon, R. E.; Schlomka, J.-P.; Fuster, V.; Fisher, E. A.; Mulder, W. J. M.; Proksa, R.; *et al.* Atherosclerotic Plaque Composition: Analysis with Multicolor CT and Targeted Gold Nanoparticles. *Radiology* **2010**, *256*, 774–782.
10. Pan, D.; Roessl, E.; Schlomka, J.-P.; Caruthers, S. D.; Senpan, A.; Scott, M. J.; Allen, J. S.; Zhang, H.; Hu, G.; Gaffney, P. J.; *et al.* Computed Tomography in Color: NanoK-Enhanced Spectral CT Molecular Imaging. *Angew. Chem., Int. Ed.* **2010**, *49*, 9635–9639.
11. Schlomka, P.; Roessl, E.; Dorscheid, R.; Dill, S.; Martens, G.; Istel, T.; Baeumer, C.; Herrmann, C.; Steadman, R.; Zeitler, G.; *et al.* Experimental Feasibility of Multi-Energy Photon-Counting K-Edge Imaging in Pre-clinical Computed Tomography. *Phys. Med. Biol.* **2008**, *53*, 4031–4047.
12. Roessl, E.; Brendel, B.; Engel, K.-J.; Schlomka, J.-P.; Thran, A.; Proksa, R. Sensitivity of Photon-Counting Based K-Edge Imaging in X-ray Computed Tomography. *IEEE Trans. Med. Imaging* **2011**, *30*, 1678–1690.
13. Krause, W.; Schumann-Gianpieri, G.; Bauer, M.; Press, W. R.; Muschick, P. Ytterbium- and Dysprosium-EOB-DTPA. A New Prototype of Liver-Specific Contrast Agents for Computed Tomography. *Invest. Radiol.* **1996**, *31*, 502–511.
14. Unger, E.; Gutierrez, F. Ytterbium-DTPA. A Potential Intravascular Contrast Agent. *Invest. Radiol* **1986**, *21*, 802–807.
15. Zwicher, C.; Heing, M.; Langer, R. Computed Tomography with Iodine-Free Contrast Media. *Eur. Radiol.* **1997**, *7*, 1123–1126.
16. Jerab, M.; Sakurai, K. Structures of Yb Nanoparticle Thin Films Grown by Deposition in He and N(2) Gas Atmospheres: AFM and X-ray Reflectivity Studies. *J. Phys.: Condens. Matter* **2010**, *22*, 474010.
17. Liu, Y.; Ai, K.; Liu, J.; Yuan, Q.; He, Y.; Lu, L. A High-Performance Ytterbium-Based Nanoparticulate Contrast Agent for *In Vivo* X-ray Computed Tomography Imaging. *Angew. Chem., Int. Ed.* **2012**, *51*, 1437–1442.
18. Schirra, C. O.; Roessl, E.; Koehler, T.; Brendel, B.; Thran, A.; Proksa, R. Maximum Likelihood CT Reconstruction from Material-Decomposed Sinograms Using Fisher Information *IEEE Nucl. Sci. Symp./MIC Conf. Proc.* **2011**, MIC21.S-45.